Available online at www.sciencedirect.com
SCIENCE DIRECT
Tetrahedron 62 (2006) 6370–6378
Tetrahedron

α-Aminoisobutyric acid modified protected analogues of β-amyloid residue 17–20: a change from sheet to helix

Debasish Haldar,[a,*] Michael G. B. Drew[b] and Arindam Banerjee[c,*]

[a]*Institut Européen de Chimie et Biologie, 2 Rue Robert Escarpit, 33607 Pessac Cedex, France*
[b]*School of Chemistry, The University of Reading, Whiteknights, Reading RG6 6AD, UK*
[c]*Department of Biological Chemistry, Indian Association for the Cultivation of Science, Jadavpur, Kolkata-700 032, India*

Received 3 January 2006; revised 29 March 2006; accepted 11 April 2006
Available online 6 May 2006

Abstract—The strong intermolecular interactions mediated by short hydrophobic sequences (e.g., 17–20, -L-Leu-L-Val-L-Phe-L-Phe-) in the middle of Aβ are known to play a crucial role in the neuropathology of Alzheimer's disease. FTIR, TEM and Congo red binding studies indicated that a series of L-Ala substituted terminally protected peptides related to the sequence 17–20 of the β-amyloid peptide, adopted β-sheet conformations. However, the Aib-modified analogues disrupt the β-sheet structure and switch over to a 3_{10} helix with increasing number of Aib residues. X-ray crystallography shed some light on the change from sheet to helix at atomic resolution.

1. Introduction

The molecular self-assembly of synthetic peptides demands special interest in advanced medicine because such molecules can serve as bioactive extra cellular materials. Self-aggregation of proteins or protein fragments is particularly important for studying pathogenesis of certain age-related diseases.[1] Though there is no similarity in native structures, sequences, length and composition of different proteins or peptides, subsequent formation of insoluble amyloid plaque is the key factor for several neurodegenerative diseases including Alzheimer's disease,[2] Huntington's disease[3] and prion protein diseases.[4] The fibrillar deposits of amyloid plaque with diameters ranging from 60 to 120 Å appeared in vivo by the transition of a misfolded protein or a peptide from its native structure to a supramolecular β-sheets arrangement.[5] For Alzheimer's disease, the Aβ peptide is generated by the proteolytic processing of a type-1 glycoprotein APP by successive β-cleavage at the N-terminus of Aβ and γ-cleavage (in the trans membrane domain) either at position 40 or 42. Moreover, APP is more frequently cleaved between amino acid 16 and 17 of the Aβ region (α-cleavage) (Fig. 1).[6] The fibrillar aggregation due to the strong intermolecular interaction of the resultant hydrophobic peptide fragments may be the direct or indirect cause of the pathological conditions associated with the amyloid diseases.[7] Some recent results demonstrate that not the matured fibrils but their precursor is pathogenic.[8] Hence, the therapeutic target is to prohibit the fibrillogenesis process.

In order to design therapeutic drugs against amyloid diseases, one of the popular approaches is the modification of amyloidogenic proteins to prevent their ability to adopt a β-sheet conformation. Previously, numerous studies have been performed using β-sheet breaking elements into short recognition sequence of amyloid protein to develop inhibitory drugs.[9] Proline and α-aminoisobutyric acid (Aib)[10] have been widely used for this purpose. Gazit et al. have

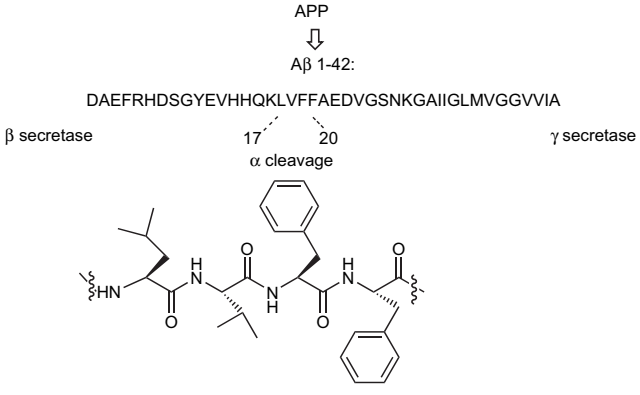

Figure 1. The sequence of amyloid β-peptide ($Aβ^{42}$) and schematic presentation of the residue 17–20 of $Aβ^{42}$. The proteolytic processing of a type-1 gycloprotein APP to generate Aβ peptide. APP is first cleaved at the N-terminus of Aβ (β-cleavage) and then in the trans membrane domain (γ-cleavage), either at position 40 or 42. Moreover, APP is more frequently cleaved between amino acid 16 and 17 of the Aβ region (α-cleavage).

Keywords: Amyloid β-peptide; Amyloid-like fibril; Aib; Supramolecular β-sheet; β-Turn; 3_{10} Helix.
* Corresponding authors. Tel.: +33 05 40002227 (D.H.); fax: +91 33 2473 2805 (A.B.); e-mail addresses: deba_h76@yahoo.com; bcab@mahendra.iacs.res.in

0040–4020/$ - see front matter © 2006 Elsevier Ltd. All rights reserved.
doi:10.1016/j.tet.2006.04.036

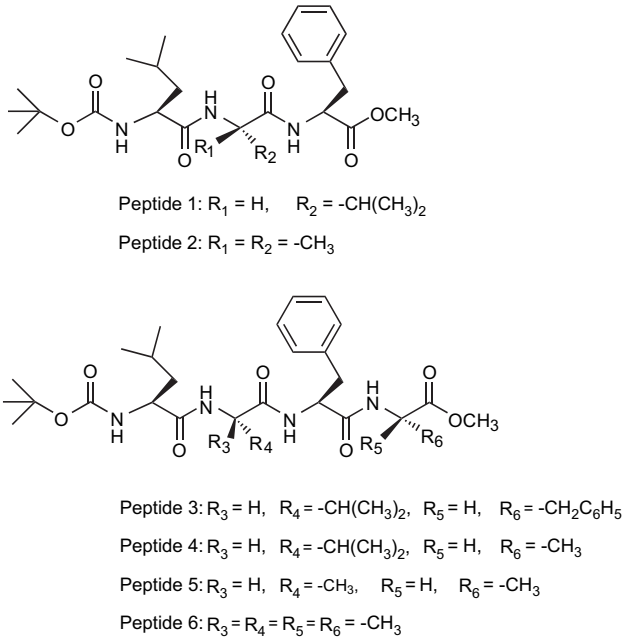

Figure 2. The schematic presentation of peptides **1**–**6**.

reported that the Aib modification of 13–20 residue of human islet amyloid polypeptide (hIPP) generates significant inhibition.[11] Formaggio and co-workers have demonstrated that the incorporation of an Aib residue into a fully protected Alzheimer's β-amyloid fragment (Aβ 17–21) can change the backbone conformation in organic solvents.[12] But all these studies depend on conventional methods like TEM and FTIR and the finer structural detail at the atomic level is still elusive.[11,12] In this context, we have synthesized some terminally protected L-Ala and Aib[13] modified analogs of Aβ 17–20 (LVFF) peptide sequences (Fig. 2). The L-Ala substituted peptides (peptides **4** and **5**) LVFA and LAFA which also have existence in the β-sheet region of corresponding protein structures (NCBI GI 5915735 (60–63) and GI 23019621 (300–303), Protein Data Bank) retain their β-sheet conformations and form amyloid-like fibrils. However, from X-ray crystallography, the Aib-modified analogues (peptide **2** and peptide **6**) disrupt the β-sheet structure and switch over to a 3_{10} helix conformation in the solid state.

2. Results and discussion

The peptides reported in this study have been synthesized using conventional solution phase methodology (Scheme 1).[14] FTIR spectra were recorded to determine the internal conformation of the reported peptides in the solid state (KBr matrix). The most informative frequency ranges are (i) 3500–3200 cm^{-1}, corresponding to the N–H stretching vibrations of the peptide and (ii) 1800–1500 cm^{-1}, corresponding to the stretching band of amide I and bending peak of amide II.[15] Figure 3 shows that molecules of the fully protected Aβ 17–20 peptides Boc-Leu-Val-Phe-OMe (**1**) and Boc-Leu-Val-Phe-Phe-OMe (**3**) have strong intermolecular H-bonds in the solid state. An intense band at 3295 cm^{-1} (peptide **1**) and 3291 cm^{-1} (peptide **3**) and a shoulder at 3328 cm^{-1} were observed for the reported peptides, indicating the presence of strongly hydrogen-bonded NH groups.[16] No band was observed at around 3400 cm^{-1}, indicating that all NH groups are involved in intermolecular hydrogen bonding.[16] The CO stretching band at 1628, 1648 cm^{-1} (amide I) and the NH bending peak at 1554, 1544 cm^{-1} (amide II) corresponding to peptides **1** and **3** suggest the presence of a β-sheet conformation in the solid state.[17] Modification of the native peptides with L-Ala produced no significant change in the infrared spectra. Peptides **4** (Boc-Leu-Val-Phe-Ala-OMe) and **5** (Boc-Leu-Ala-Phe-Ala-OMe) have peaks at 3316 and 3289 cm^{-1}, which might indicate the presence of intermolecular hydrogen-bonded NH groups (Fig. 4). Moreover, the characteristic IR absorption bands at about 1642 and 1640 cm^{-1} (amide I)

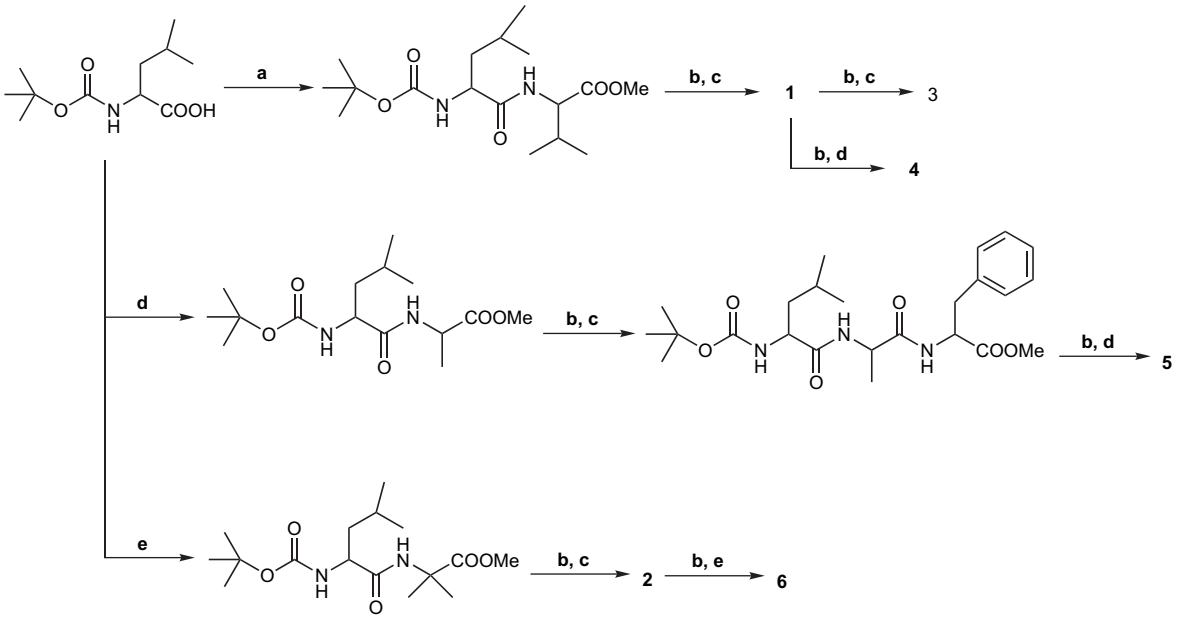

Scheme 1. Reagents and conditions: (a) DMF, H-Val-OMe, DCC, HOBt, 0 °C, 90% yield; (b) MeOH, 2 M NaOH, 85% yield; (c) DMF, H-Phe-OMe, DCC, HOBt, 0 °C, 80% yield; (d) DMF, H-Ala-OMe, DCC, HOBt, 0 °C, 80% yield; (e) DMF, H-Aib-OMe, DCC, HOBt, 0 °C, 90% yield.

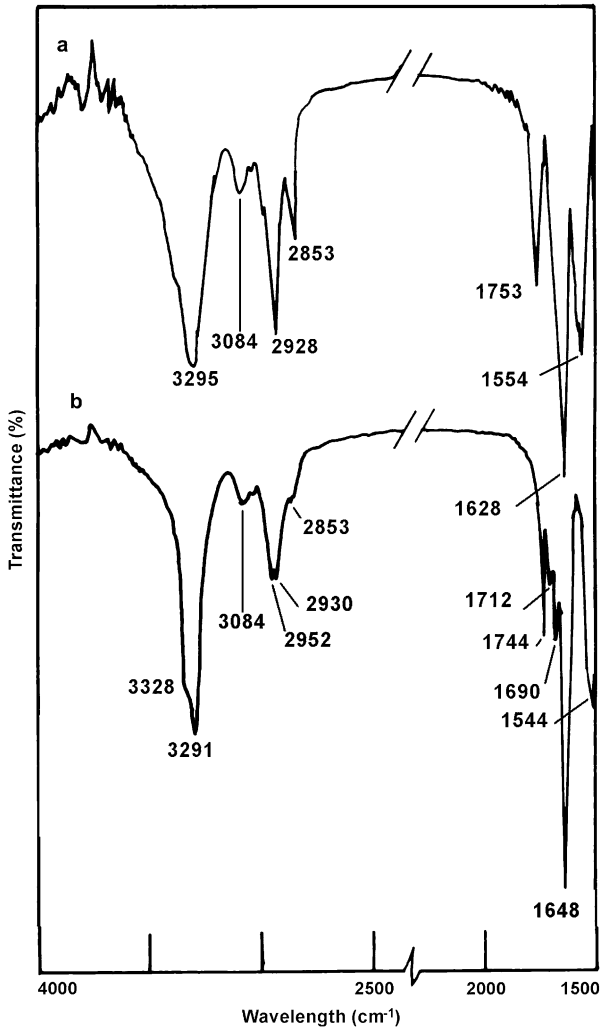

Figure 3. Solid state FTIR spectra of (a) peptide **1** and (b) peptide **3** at the region 2500–4000 cm^{-1} and 1500–2000 cm^{-1}.

and 1530 and 1546 cm^{-1} (amide II) of peptides **4** and **5**, respectively, suggest that the peptides have spectra typical of β-sheet structures.[15,17] Therefore, this very minor chemical modification (replacement of amino acid residues 2 and 4 of peptide **3** by L-Ala) results in little effect on the amyloidogenic potential of the native peptide. But the Aib-modified peptides produce significant changes (1659 and 1661 cm^{-1} (amide I) for peptide **2** and **6**), which are consistent with the previous report.[11,18]

Further, we examined the ability of the L-Ala modified peptides to form amyloid-like fibrils, compared to that of native peptides. Although the overall changes in the chemical structures are minor, we observed no differences between the abilities of the native and modified peptides to form amyloid-like fibrils. The amyloidogenic nature of the peptides was determined by transmission electron microscopy (TEM). The TEM was performed on both transmission mode and diffraction mode. From the TEM images of these peptides, it is evident that they share a common morphological property irrespective of the difference in sequences. Figure 5 clearly shows that peptide **4** exhibits amyloid-like tangles with multiple branching nodes, a very common feature of amyloid plaque obtained from many neurodegenerative diseases. From the transmission

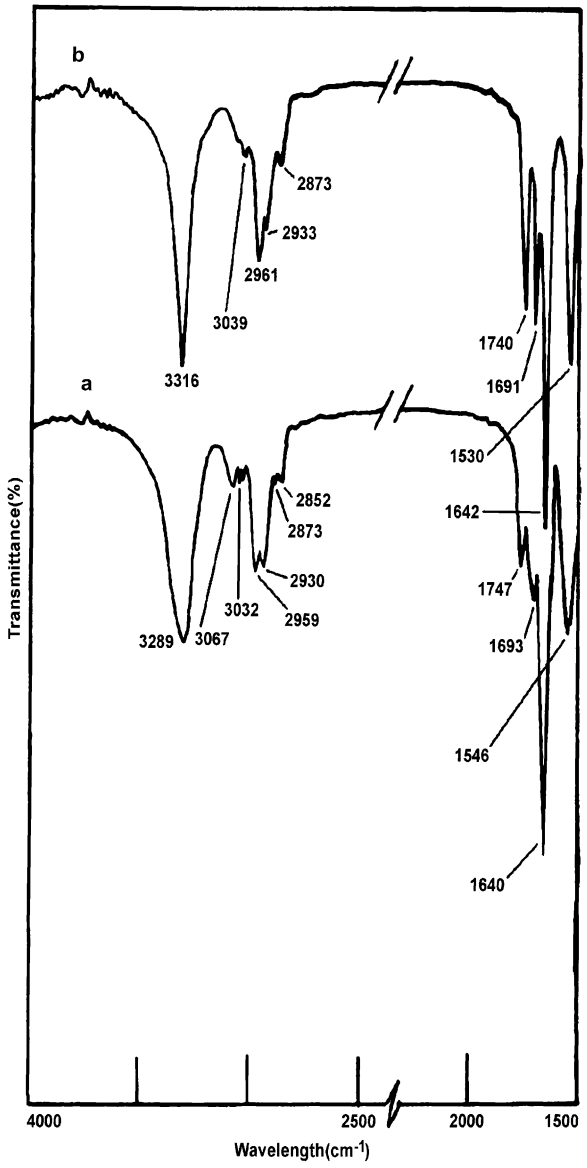

Figure 4. FTIR spectra at the region 2500–4000 cm^{-1} and 1500–2000 cm^{-1} of (a) peptide **5** and (b) peptide **4** in the solid state.

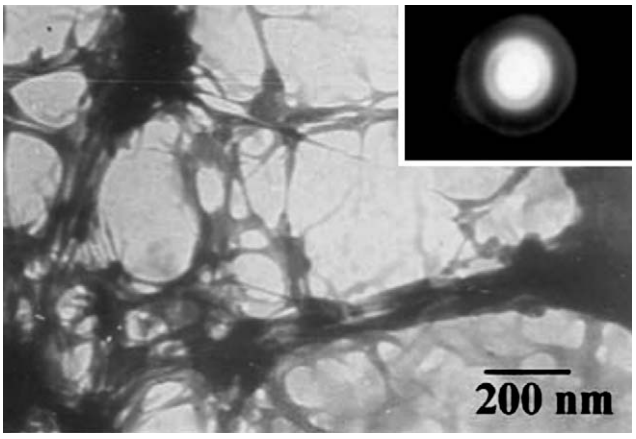

Figure 5. Electron microscopy and electron diffraction (inset) (0.5% w/v) of peptide **4**. Transmission electron micrograph of peptide **4** showing amyloid-like tangles and multiple branching nodes.

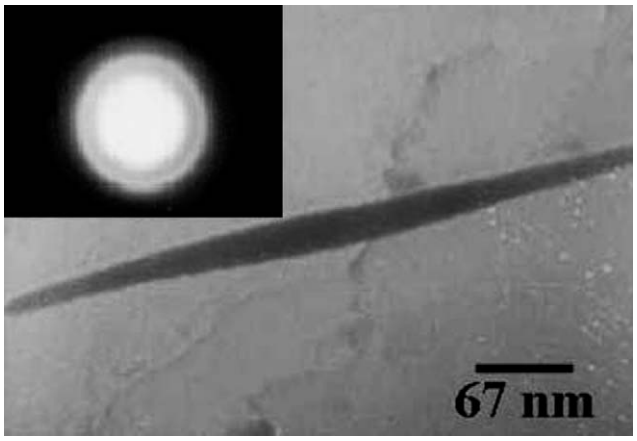

Figure 6. Transmission electron microscopy and electron diffraction (inset) (0.5% w/v) of peptide **5**. The TEM image exhibits filamentous fibrillar morphology.

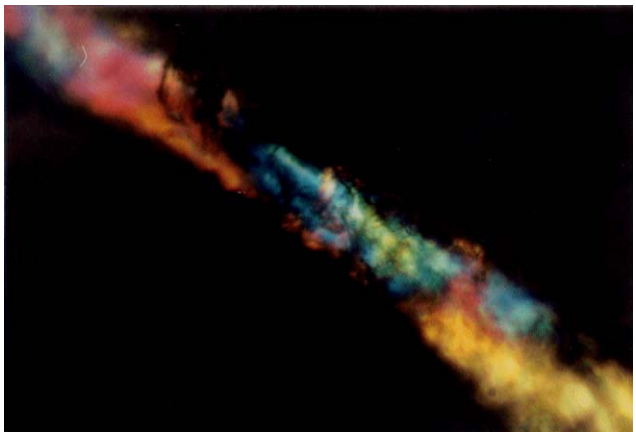

Figure 8. Congo red stained peptide **5** fibrils observed through crossed polarizer showing green-gold birefringence, a characteristic feature of amyloid fibrils.

electron micrograph, peptide **5** aggregates like a bundle of long filaments, reminiscent of amyloid fibrils (Fig. 6). However, the transmission electron micrograph of the corresponding Aib analogue (peptide **6**) shows nanorod[19]-like structures with diameters ranging from 60 to 70 nm in the solid state (Fig. 7).

The morphological resemblance of these peptide fibrils with amyloid plaque was also studied by Congo red staining. It has been reported that Congo red binds with amyloid fibrils responsible for various neurodegenerative diseases like Alzheimer's disease and shows a distinct birefringence under polarized light. To determine the similarity with Alzheimer's β-amyloid fibrils, the aggregated fibrils obtained from these peptides were stained with Congo red and observed through a cross polarizer. Figure 8 exhibits the typical green-gold birefringence of Congo red bound fibrils of peptide **5** under cross polarizer, similar to the native peptides. These results are consistent with Congo red binding to an amyloid β-sheet fibrillar structure.[7a,b,d] We conclude that there is almost no difference between native peptides, which are highly amyloidogenic and their L-Ala containing analogues. But the aggregate obtained from Aib-modified analogue peptide **6** does not exhibit typical birefringence when stained with Congo red and viewed through cross polarizers under same conditions (Fig. 9).

However, from X-ray crystallography, the modification of the native peptides to Aib-containing peptides produced a significant change in the peptide backbone conformations.[20] Most of the ϕ and ψ values of the constituent amino acid residues of peptide **2**, an Aib analogue of native peptide **1**, fall within the helical region of the Ramachandran map. The torsion angles ϕ_1 (−62.91) and ψ_1 (−41.20) are in the right-handed helical region whereas the ϕ_2 (58.15) and ψ_2 (46.24) are in the left-handed helical region. There is also a distortion for ϕ_3 (−55.3) and ψ_3 (141.4), which prevents the peptide from forming any intramolecular hydrogen-bonded folded structures. Hence, the overall backbone conformation is a helical one in comparison with the native peptides (Fig. 10a).[20a] However, with an increasing number of Aib residues, the peptide backbone completely switches over into a 3_{10} helical conformation. Peptide **6** contains two alternating Aib residues and forms a consecutive β-turn (10 member intramolecular hydrogen-bonded ring) structure where the Aib(2) occupies the *i*+2th position of first turn and *i*+1th position of the second turn (Fig. 10b). From Figure 10b, there are two intramolecular hydrogen bonds N4–H4···O11 (2.21 Å, 2.94 Å, 143°) and N7–H7···O14 (2.41 Å, 3.26 Å, 169°) resulting in a consecutive double bend conformation for individual peptide (**6**) molecules in the solid state. Most of the backbone torsion angles [ϕ_1(−70.2°), ψ_1(−16.9°),

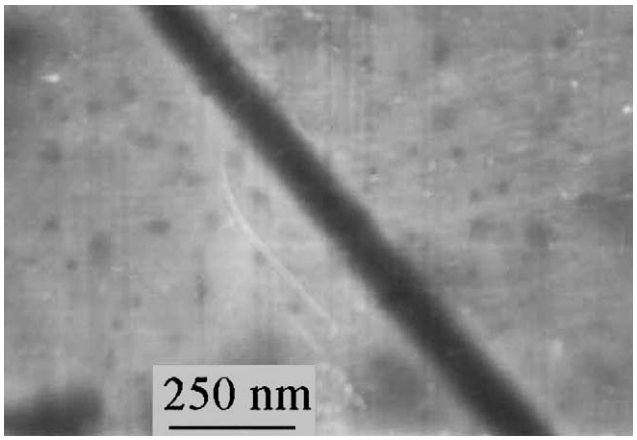

Figure 7. Transmission electron micrographs of peptide **6** showing nanorod-like morphology in the solid state.

Figure 9. Peptide **6** stained with Congo red dye fails to show any birefringence observed between cross polarizer.

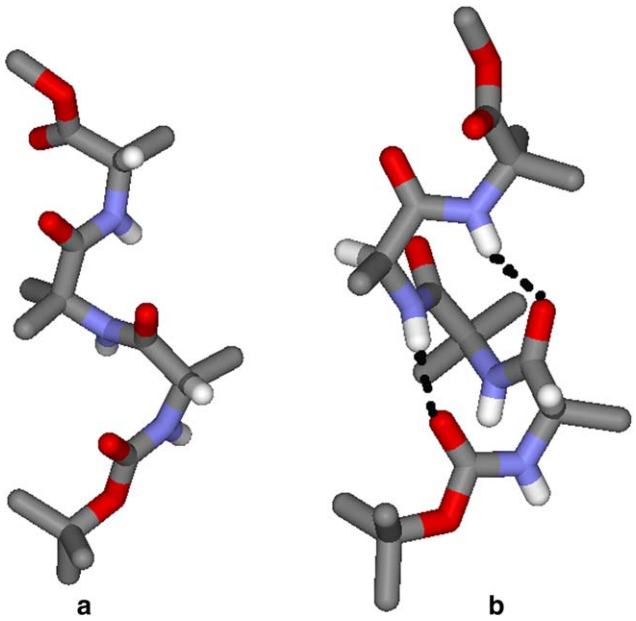

Figure 10. The molecular backbone conformation of (a) peptide **2** and (b) peptide **6** showing a 3_{10} helical switch over from peptide **2** to **6**. Intramolecular hydrogen bonds are shown as dotted line. The side chains for Leu and Phe residues and other non-hydrogen-bonded hydrogen atoms are omitted for clarity. Nitrogen atoms are blue, oxygen atoms are red and carbon atoms are gray.

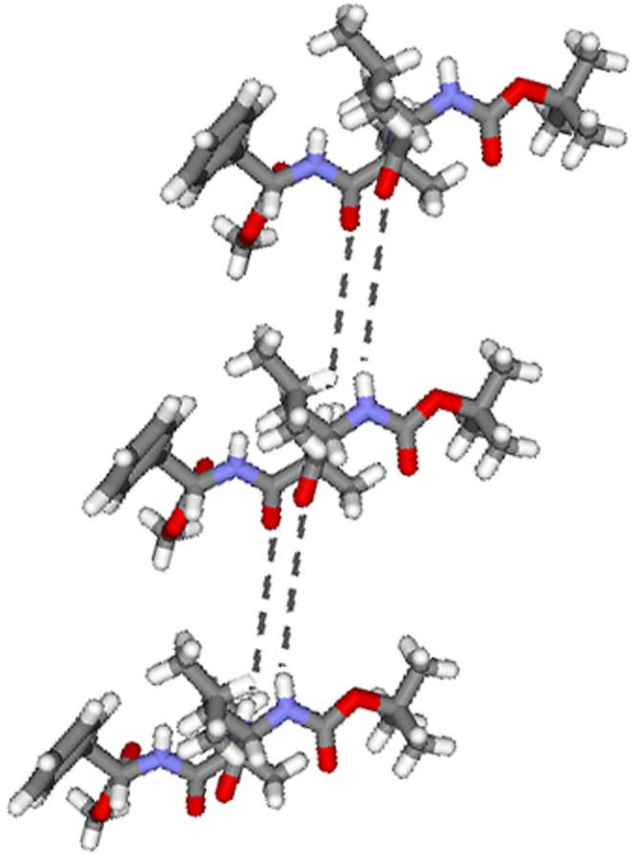

Figure 11. The packing of peptide **2** along crystallographic *a*-axis showing multiple intermolecular hydrogen bonds that connect individual molecules to form parallel sheet-like structure. Hydrogen bonds are shown as dotted line.

$\phi_2(-57.8°)$, $\psi_2(-21.3°)$, $\phi_3(-56.4°)$ and $\psi_3(-35.9°)$] of peptide **6** are in the 3_{10} helical region of Ramachandran diagram [except $\phi(51.3°)$ and $\psi(-135.7°)$ values of Aib(4)].[20b] Thus, there is a distinct conformational change from the native peptide to its Aib analogues. The peptide backbone changes from a β-sheet structure of the native peptide to the 3_{10} helical conformations in the Aib-modified peptide.

Moreover, in higher order packing, two intermolecular hydrogen bonds N4–H4···O3 (2.27 Å, 3.08 Å, 158°) and N6–H62···O5 (2.10 Å, 2.98 Å, 147°) connect individual molecules of peptide **2** to form a parallel sheet-like structure (Fig. 11) along crystallographic *a*-axis. Therefore, peptide **2** preserves some characteristics of the native peptides instead of the incorporation of an Aib residue. But, the individual sub-units of the 3_{10} helical peptide **6** are themselves regularly inter-linked via multiple intermolecular hydrogen bonds N10–H10···O5 (2.20 Å, 2.99 Å, 152°) and N13–H13···O8 (2.30 Å, 3.15 Å, 170°) and thereby form a supramolecular helix along the crystallographic *b*-direction (Fig. 12). This very minor chemical modification results in such a dramatic effect on the molecular backbone

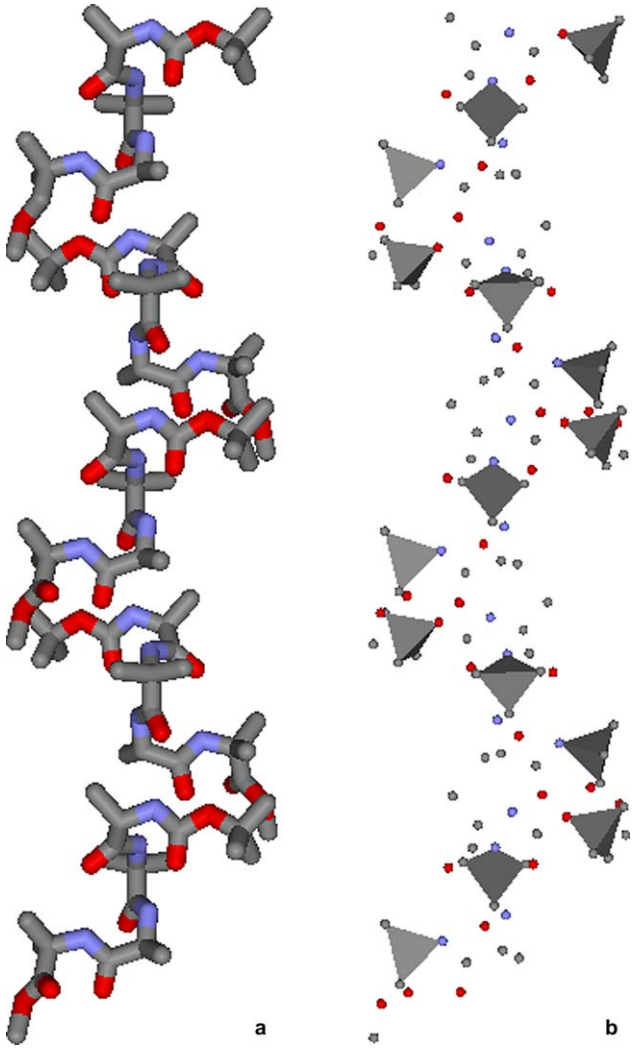

Figure 12. The packing diagram of peptide **6** showing the intermolecular hydrogen bonded supramolecular helix along the crystallographic *b*-direction in (a) stick and (b) polyhedron representation.

Table 1. Crystal and data collection parameters of peptides **2** and **6**

	Peptide **2**	Peptide **6**
Empirical formula	$C_{25}H_{39}N_3O_6$	$C_{29}H_{45}N_4O_7$
Crystallizing solvent	Dimethyl sulfoxide	Ethyl acetate
Crystal system	Orthorhombic	Orthorhombic
Space group	$P2_12_12_1$	$P2_12_12_1$
a (Å)	6.023(3)	13.253(17)
b (Å)	10.311(3)	15.694(19)
c (Å)	43.051(7)	15.768(19)
α (°)	90	90
β (°)	90	90
γ (°)	90	90
v (Å^3)	2673.6(16)	3280(7)
μ (Mo Kα)/mm	0.085	0.081
Z	4	4
Mol. wt.	477.59	561.69
Density (calcd, mg/mm^3)	1.186	1.137
F(000)	1032	1212
T (°)	293	293
Tot., uniq. data	4509, 4179	3474, 3474
Observed reflns. $I>2\sigma(I)$	2887	1716
R	0.0577	0.0624
wR	0.1983	0.1800
S	1.22	0.98
λ (Å) (Mo Kα)	0.71073	0.71073
No. of param.	340	372

conformation and nature of the native peptides. Crystal data for peptides **2** and **6** are listed in Table 1.

3. Conclusion

In conclusion, it is clearly established that the L-Ala substituted analogue of the fully protected peptides related to the sequence 17–20 of amyloid β peptide have almost similar characteristics in comparison to the native peptides, which are highly amyloidogenic. Moreover, the β-sheet structure of the native peptides is completely disrupted by the incorporation of a conformationally constrained α-aminoisobutyric acid. From X-ray crystallography, it is unambiguously demonstrated that there is a distinct change from β-sheet to 3_{10} helix conformations in the Aib modification of the native peptides. These results will be useful in efforts to design peptide-based inhibitors of amyloid fibrillogenesis to prevent various neurodegenerative diseases.

4. Experimental

4.1. Synthesis of the peptides

4.1.1. Boc-Leu-OH 7. See Ref. 21.

4.1.2. Boc-Leu-Val-OMe 8. See Ref. 22.

4.1.3. Boc-Leu-Val-OH 9. See Ref. 22.

4.1.4. Boc-Leu-Val-Phe-OMe 1. See Ref. 23.

4.1.5. Boc-Leu-Val-Phe-OH 10. To Boc-Leu-Val-Phe-OMe (9.82 g, 20 mmol), methanol (50 mL) and 2 M NaOH (20 mL) were added and the progress of saponification was monitored by thin layer chromatography (TLC). The reaction mixture was stirred at room temperature. After 10 h, methanol was removed under vacuum, the residue was taken in 50 mL of water, washed with diethyl ether (2×50 mL). Then, pH of the aqueous layer was adjusted to 2 by adding 1 M HCl and it was extracted with ethyl acetate (3× 40 mL). The extracts were pooled, dried over anhydrous sodium sulfate and evaporated under vacuum to yield a white waxy solid.

Yield=80% (7.64 g, 16 mmol). ^{1}H NMR (DMSO-d_6, 300 MHz): δ 12.37 (br, 1H), 8.27 (d, J=7.5 Hz, 1H), 7.46 (d, J=9.1 Hz, 1H), 7.19–7.27 (m, 5H), 7.05 (d, J=8.5 Hz, 1H), 4.42 (m, 1H), 4.20 (m, 1H), 3.94 (m, 1H), 3.02 (m, 2H), 2.88 (m, 1H), 1.92 (m, 2H), 1.36 (s, 9H), 0.87 (d, J= 6.9 Hz, 6H), 0.76–0.84 (m, 7H) ppm. ^{13}C NMR ($CDCl_3$, 300 MHz): δ 11.24, 11.47, 18.18, 22.37, 22.93, 22.98, 24.82, 28.14, 31.17, 35.03, 41.38, 52.23, 52.26, 58.43, 80.16, 127.14, 128.47, 129.15, 135.81, 170.18, 170.81, 171.69, 176.25 ppm. $[\alpha]_D^{27.8}$ −19.9 (c 2.10, $CHCl_3$). Elemental Anal. Calcd for $C_{25}H_{39}N_3O_6$ (477): C, 62.89; H, 8.18; N, 8.80. Found: C, 63.21; H, 8.36; N, 7.94.

4.1.6. Boc-Leu-Val-Phe-Phe-OMe 3. The mixture of **10** (4.77 g, 10 mmol) in DMF (20 mL) was cooled in an ice-water bath. H-Phe-OMe was isolated from the corresponding methyl ester hydrochloride (4.33 g, 20 mmol) by neutralization with saturated $NaHCO_3$ solution, subsequent extraction with ethyl acetate and the ethyl acetate extract was concentrated to 20 mL. This was added to the reaction mixture, followed immediately by DCC (2 g, 10 mmol) and HOBt (1.4 g, 10 mmol). The reaction mixture was stirred for 3 days. The residue was taken in ethyl acetate (50 mL) and DCU was filtered off. The organic layer was washed with 2 M HCl (3×50 mL), brine, 1 M sodium carbonate (3× 50 mL), brine (2×50 mL), dried over anhydrous sodium sulfate and evaporated in vacuum to get a white solid.

Yield=80% (5.1 g, 8 mmol). Mp 153–154 °C. IR (KBr): 1544, 1648, 1690, 1744, 2853, 2930, 2952, 3084, 3291, 3328 cm^{-1}. ^{1}H NMR ($CDCl_3$, 300 MHz): δ 7.22–7.26 (m, 10H), 7.02 (d, J=6.9 Hz, 1H), 6.62 (d, J=7.8 Hz, 1H), 6.53 (d, J=7.1 Hz, 1H), 4.83 (d, J=8.3 Hz, 1H), 4.78 (m, 1H), 4.74 (m, 1H), 4.14 (m, 1H), 4.03 (m, 1H), 3.66 (s, 3H), 2.94–3.13 (m, 4H), 2.14 (m, 1H), 1.94 (m, 2H), 1.44 (s, 9H), 0.96 (d, J=6.6 Hz, 6H), 0.74–0.85 (m, 7H) ppm. ^{13}C NMR ($CDCl_3$, 300 MHz): δ 11.23, 11.49, 18.23, 22.35, 22.91, 22.99, 24.83, 28.14, 31.13, 35.07, 36.88, 41.33, 51.71, 52.33, 52.19, 58.47, 80.18, 127.14, 128.47, 129.15, 135.81, 170.20, 170.80, 171.69, 171.84, 173.35 ppm. $[\alpha]_D^{27.8}$ −35.7 (c 2.10, $CHCl_3$). Mass spectral data $(M+Na)^+$=661.60, M_{calcd}=638. Elemental Anal. Calcd for $C_{35}H_{50}N_4O_7$ (638): C, 65.83; H, 7.84; N, 8.78. Found: C, 65.34; H, 7.51; N, 10.16.

4.1.7. Boc-Leu-Val-Phe-Ala-OMe 4. The Boc-Leu-Val-Phe-OH (2.40 g, 5 mmol) in DMF (10 mL) was cooled in an ice-water bath. H-Ala-OMe was isolated from the corresponding methyl ester hydrochloride (1.4 g, 10 mmol) by neutralization with saturated $NaHCO_3$ solution, subsequent extraction with ethyl acetate and the ethyl acetate extract was then concentrated to 7 mL. This was added to the reaction mixture, followed immediately by DCC (1 g, 5 mmol) and HOBt (0.7 g, 5 mmol). The reaction mixture was stirred for 3 days. The residue was taken in ethyl acetate (50 mL) and DCU was filtered off. The organic layer was washed

with 2 M HCl (3×50 mL), brine, 1 M sodium carbonate (3×50 mL), brine (2×50 mL), dried over anhydrous sodium sulfate and evaporated under vacuum to get 1.97 g of white solid.

Yield=70% (1.97 g, 3.5 mmol). Mp 144–145 °C. IR (KBr): 1530, 1642, 1691, 1740, 2933, 2961, 3039, 3316 cm^{-1}. ^1H NMR ($CDCl_3$, 300 MHz): δ 7.22–7.26 (m, 5H), 7.19 (d, J=6.9 Hz, 1H), 6.75 (d, J=8.4 Hz, 1H), 6.70 (d, J=7.5 Hz, 1H), 4.91 (d, J=6.0 Hz, 1H), 4.80 (m, 1H), 4.50 (m, 1H), 4.16 (m, 1H), 4.06 (m, 1H), 3.71 (s, 3H), 3.01 (m, 2H), 2.15 (m, 1H), 1.93 (m, 2H), 1.44 (s, 9H), 1.37 (d, J=7.2 Hz, 3H), 0.95 (m, 6H), 0.74–0.87 (m, 7H) ppm. ^{13}C NMR ($CDCl_3$, 300 MHz): δ 11.16, 11.29, 18.99, 22.33, 22.82, 22.97, 24.79, 24.83, 28.14, 31.13, 35.07, 41.35, 51.71, 52.13, 52.19, 58.47, 80.17, 127.14, 128.47, 129.15, 135.81, 170.24, 170.87, 171.73, 171.81, 172.25 ppm. $[\alpha]_D^{27.8}$ −42.2 (c 2.10, $CHCl_3$). Mass spectral data (M+Na+2H)$^+$=587.20, M_{calcd}=562. Elemental Anal. Calcd for $C_{29}H_{46}N_4O_7$ (562): C, 61.92; H, 8.18; N, 9.96. Found: C, 61.49; H, 7.81; N, 10.26.

4.1.8. Boc-Leu-Ala-OMe 11. See Ref. 24.

4.1.9. Boc-Leu-Ala-OH 12. See Ref. 25.

4.1.10. Boc-Leu-Ala-Phe-OMe 13. See Ref. 26.

4.1.11. Boc-Leu-Ala-Phe-OH 14. To Boc-Leu-Ala-Phe-OMe (3.70 g, 8 mmol), methanol (50 mL) and 2 M NaOH (20 mL) were added and the progress of saponification was monitored by thin layer chromatography (TLC). The reaction mixture was stirred at room temperature. After 10 h, methanol was removed under vacuum, the residue was taken in water (50 mL), washed with diethyl ether (2×50 mL). Then, pH of the aqueous layer was adjusted to 2 by adding 1 M HCl and it was extracted with ethyl acetate (3×40 mL). The extracts were pooled, dried over anhydrous sodium sulfate and evaporated under vacuum to yield a waxy solid.

Yield=87% (3.14 g, 7 mmol). ^1H NMR (DMSO-d_6, 300 MHz): δ 12.1 (br, 1H), 7.20–7.27 (m, 5H), 8.02 (d, J=7.5 Hz, 1H), 7.85 (d, J=7.9 Hz, 1H), 6.80 (d, J=8.8 Hz, 1H), 4.40 (m, 1H), 3.97 (m, 1H), 3.86 (m, 1H), 3.10 (m, 2H), 2.88 (d, J=4.4 Hz, 3H), 2.50 (m, 2H), 1.36 (s, 9H), 0.80–0.90 (m, 7H) ppm. ^{13}C NMR ($CDCl_3$, 300 MHz): δ 11.35, 11.57, 18.19, 22.37, 22.93, 24.79, 24.82, 28.14, 31.17, 41.38, 52.23, 52.26, 58.43, 80.16, 127.14, 128.47, 129.15, 135.81, 170.18, 170.80, 171.71, 176.35 ppm. $[\alpha]_D^{27.8}$ −15.3 (c 2.10, $CHCl_3$). Elemental Anal. Calcd for $C_{23}H_{35}N_3O_6$ (449): C, 61.47; H, 7.79; N, 9.35. Found: C, 61.85; H, 8.16; N, 8.89.

4.1.12. Boc-Leu-Ala-Phe-Ala-OMe 5. The mixture of **14** (2.24 g, 5 mmol) in DMF (10 mL) was cooled in an ice-water bath. H-Ala-OMe was isolated from the corresponding methyl ester hydrochloride (1.40 g, 10 mmol) by neutralization with saturated $NaHCO_3$ solution, subsequent extraction with ethyl acetate and the ethyl acetate extract was concentrated to 7 mL. This was added to the reaction mixture, followed immediately by DCC (1 g, 5 mmol) and HOBt (0.70 g, 5 mmol). The reaction mixture was stirred for 3 days. The residue was taken in ethyl acetate (50 mL) and DCU was filtered off. The organic layer was washed with 2 M HCl (3×50 mL), brine, 1 M sodium carbonate (3×50 mL), brine (2×50 mL), dried over anhydrous sodium sulfate and evaporated in vacuum to get 2.14 g (4 mmol) of white solid.

Yield=80% (2.14 g, 4 mmol). Mp 161–162 °C. IR (KBr): 1546, 1640, 1693, 1747, 2930, 2959, 3032, 3289 cm^{-1}. ^1H NMR ($CDCl_3$, 300 MHz): δ 7.24–7.27 (m, 5H), 7.18 (d, J=8.4 Hz, 1H), 6.72 (d, J=9.4 Hz, 1H), 6.66 (d, J=9.4 Hz, 1H), 4.99 (d, J=7.1 Hz, 1H), 4.63 (m, 1H), 4.00 (m, 2H), 3.80 (m, 1H), 3.72 (s, 3H), 3.17 (m, 2H), 3.03 (m, 2H), 1.44 (s, 9H), 1.36 (d, J=7.2 Hz, 6H), 0.89–0.96 (m, 7H) ppm. ^{13}C NMR ($CDCl_3$, 300 MHz): δ 11.23, 11.49, 18.95, 22.36, 22.80, 22.99, 24.74, 24.80, 28.16, 31.23, 35.09, 41.25, 51.69, 52.11, 52.20, 58.47, 80.18, 127.14, 128.47, 129.15, 135.81, 170.24, 170.85, 171.73, 171.80, 172.25 ppm. $[\alpha]_D^{27.8}$ −52.7 (c 2.10, $CHCl_3$). Mass spectral data (M+Na)$^+$=557.70, M_{calcd}=534. Elemental Anal. Calcd for $C_{27}H_{42}N_4O_7$ (534): C, 60.67; H, 7.86; N, 10.49. Found: C, 60.43; H, 7.25; N, 10.07.

4.1.13. Boc-Leu-Aib-OMe 15. See Ref. 27.

4.1.14. Boc-Leu-Aib-OH 16. See Ref. 27.

4.1.15. Boc-Leu-Aib-Phe-OMe 2. Boc-Leu-Aib-OH (6.06 g, 20 mmol) in DMF (20 mL) was cooled in an ice-water bath and H-Phe-OMe was isolated from the corresponding methyl ester hydrochloride (8.62 g, 40 mmol) by neutralization with saturated $NaHCO_3$ solution, subsequent extraction with ethyl acetate and the ethyl acetate extract was concentrated to 10 mL. It was added to the reaction mixture, followed immediately by DCC (4.12 g, 20 mmol) and HOBt (2.70 g, 20 mmol). The reaction mixture was stirred for 3 days. The residue was taken in ethyl acetate (60 mL) and the DCU was filtered off. The organic layer was washed with 2 M HCl (3×50 mL), brine, 1 M sodium carbonate (3×50 mL), brine (2×50 mL), dried over anhydrous sodium sulfate and evaporated under *vacuum* to yield 8.11 g (17 mmol) of white solid. Purification was achieved by silica gel column (100–200 mesh) using ethyl acetate and toluene mixture (1:2) as an eluent. Single crystals were grown from dimethyl sulfoxide (DMSO) mixture by slow evaporation.

Yield=81% (8.11 g, 17 mmol). Mp 115–117 °C. IR (KBr): 1659, 1697, 3321, 3421 cm^{-1}. ^1H NMR ($CDCl_3$, 500 MHz): δ 7.22–7.30 (m, 5H), 7.13 (d, J=7.8 Hz, 1H), 6.89 (d, J=6.8 Hz, 1H), 6.61 (s, 1H), 4.81 (m, 1H), 3.98 (m, 1H), 3.70 (s, 3H), 3.11 (m, 2H), 1.60 (m, 2H), 1.49 (s, 9H), 1.44 (s, 6H), 1.25 (m, 1H), 0.94 (m, 6H) ppm. ^{13}C NMR ($CDCl_3$, 300 MHz): δ 11.31, 11.49, 15.33, 18.18, 22.37, 24.38, 24.82, 28.04, 31.17, 37.03, 51.23, 56.26, 58.43, 80.24, 127.54, 129.06, 129.15, 136.81, 170.60, 170.80, 171.84, 173.58 ppm. $[\alpha]_D^{27.8}$ +5.3 (c 2.10, $CHCl_3$). Mass spectral data (M+Na)$^+$=500, M_{calcd}=477. Elemental Anal. Calcd for $C_{25}H_{39}N_3O_6$ (477): C, 62.89; N, 8.80; H, 8.17. Found: C, 63.06; N, 8.87; H, 7.90.

4.1.16. Boc-Leu-Aib-Phe-OH 17. To Boc-Leu-Aib-Phe-OMe (4.77 g, 10 mmol), methanol (50 mL) and 2 M NaOH (20 mL) were added and the progress of saponification was

monitored by thin layer chromatography (TLC). The reaction mixture was stirred at room temperature. After 10 h methanol was removed under vacuum, the residue was taken in water (50 mL), washed with diethyl ether (2×50 mL). Then, the pH of the aqueous layer was adjusted to 2 by adding 1 M HCl and it was extracted with ethyl acetate (3×40 mL). The extracts were pooled, dried over anhydrous sodium sulfate and evaporated under vacuum to yield a waxy solid.

Yield=70% (3.24 g, 7 mmol). ^{1}H NMR (DMSO-d_6, 300 MHz): δ 12.56 (br, 1H), 7.85 (s, 1H), 7.47 (d, J=5.4 Hz, 1H), 7.23–7.13 (m, 5H), 6.90 (d, J=7.56 Hz, 1H), 4.36 (m, 1H), 3.85 (m, 1H), 2.86 (m, 2H), 1.56 (m, 2H), 1.34 (s, 9H), 1.26 (s, 6H), 0.84–0.80 (m, 7H) ppm. ^{13}C NMR ($CDCl_3$, 300 MHz): δ 11.23, 11.47, 15.31, 18.16, 22.37, 24.38, 24.82, 28.04, 31.17, 37.03, 56.26, 58.43, 80.24, 127.54, 129.06, 129.15, 136.81, 170.69, 170.78, 171.81, 176.25 ppm. $[\alpha]_D^{27.8}$ −5.7 (c 2.10, $CHCl_3$). Elemental Anal. Calcd for $C_{24}H_{37}N_3O_6$ (463): C, 62.20; H, 7.99; N, 9.07. Found: C, 62.05; H, 8.16; N, 8.89

4.1.17. Boc-Leu-Aib-Phe-Aib-OMe 6. Boc-Leu-Aib-Phe-OH (2.32 g, 5 mmol) in DMF (10 mL) was cooled in an ice-water bath. H-Aib-OMe was isolated from the corresponding methyl ester hydrochloride (1.53 g, 10 mmol) by neutralization with saturated $NaHCO_3$, subsequent extraction with ethyl acetate and the ethyl acetate extract was then concentrated to 7 mL. This was added to the reaction mixture, followed immediately by DCC (1 g, 5 mmol) and HOBt (0.7 g, 5 mmol). The reaction mixture was stirred for 3 days. The residue was taken in ethyl acetate (50 mL) and DCU was filtered off. The organic layer was washed with 2 M HCl (3×50 mL), brine, 1 M sodium carbonate (3×50 mL), brine (2×50 mL), dried over anhydrous sodium sulfate and evaporated under vacuum to get white solid. Purification was done by silica gel column (100–200 mesh) using ethyl acetate as an eluent. Single crystals were obtained from ethyl acetate solution by slow evaporation.

Yield=80% (2.25 g, 4 mmol). Mp 141–142 °C. IR (KBr): 1661, 1728, 3273, 3341 cm^{-1}. ^{1}H NMR ($CDCl_3$, 300 MHz): δ 7.19–7.26 (m, 5H), 7.17 (s, 1H), 6.74 (d, J=8.1 Hz, 1H), 6.49 (s, 1H), 4.79 (d, J=5.1 Hz, 1H), 4.75 (m, 1H), 3.87 (m, 1H), 3.72 (s, 3H), 3.43 (m, 2H), 2.94 (m, 2H), 1.52 (s, 6H), 1.48 (s, 6H), 1.45 (s, 9H), 0.93 (m, 7H) ppm. ^{13}C NMR ($CDCl_3$, 300 MHz): δ 11.49, 11.57, 15.47, 18.18, 22.37, 24.38, 24.82, 28.04, 31.17, 37.03, 52.03, 56.26, 57.43, 80.24, 128.54, 129.06, 129.15, 155.82, 170.37, 171.80, 173.84, 174.89 ppm. $[\alpha]_D^{27.8}$ −17.6 (c 2.10, $CHCl_3$). Mass spectral data $(M+Na)^+$=585.4, M_{calcd}=462. Elemental Anal. Calcd for $C_{29}H_{46}N_4O_7$ (562): C, 61.81; H, 8.35; N, 9.95. Found: C, 61.03; H, 8.57; N, 9.19.

4.2. NMR experiments

All NMR studies were carried out on Brüker DPX 300 and DRX 500 MHz spectrometer at 300 K in $CDCl_3$ and DMSO-d_6. Peptide concentrations were in the range 1–10 mM.

4.3. Mass spectrometry

Mass spectra of peptides were recorded on a Micromass Zabspec Hybrid Sector-TOF by positive mode electronspray ionization using a 1% solution of acetic acid in methanol/water as liquid carrier.

4.4. FTIR spectroscopy

The FTIR spectra were taken using Shimadzu (Japan) model FTIR spectrophotometer. The solid-state FTIR measurements were performed using the KBr disk technique.

4.5. Morphological studies

Morphologies of the reported compounds were investigated using transmission electron microscopy (TEM). The transmission electron microscopic studies of these peptides were performed using a small amount of the solution of the corresponding compound on carbon-coated copper grids (200 mesh) by slow evaporation and allowed to dry in vacuum at 30 °C for 2 days. Images were taken at an accelerating voltage of 100 kV both in the transmission mode and diffraction mode (0.5% w/v, camera length 0.8 m). TEM was done by a Hitachi 600 electron microscope.

4.6. Congo red binding study

An alkaline saturated Congo red solution was prepared. The peptide fibrils were stained by alkaline Congo red solution (80% methanol/20% glass distilled water containing 10 mL of 1% NaOH) for 2 min and then the excess stain (Congo red) was removed by rinsing the stained fibril with 80% methanol/20% glass distilled water solution for several times. The stained fibrils were dried in vacuum at room temperature for 24 h, then visualized at 100× or 500× magnification and birefringence was observed between crossed polarizer.

4.7. Single crystal X-ray diffraction studies

For peptide **2**, intensity data of orthorhombic colorless crystals 0.48×0.52×0.65 of space group $P2_12_12_1$ were collected with Mo Kα radiation, ω scan using graphite-monochromated Siemens P4 diffractometer. The crystal was positioned at 70 mm from the image plate. One hundred frames were measured at 2° intervals with a counting time of 2 min to give 4179 independent reflections of which 2887 had $I>2\sigma(I)$. The structure was solved by direct methods (SHELXS-97)[28] and refined against F(obs)×2 by full-matrix least squares (SHELXL-97).[29] Hydrogen atoms were placed at calculated positions and allowed to ride on their parent atoms. Terminal reliability indices were $R1$=0.058 [$I>2\sigma(I)$], $wR2$=0.198 for 340 refined parameters, S=1.21, min./max. res. 0.19/−0.19 eÅ^{-3}.

For peptide **6**, intensity data were collected with Mo Kα radiation using the MAR research Image Plate System. The crystal was positioned at 70 mm from the image plate. One hundred frames were measured at 2° intervals with a counting time of 5 min to give 3474 independent reflections. Data analysis was carried out with the XDS program.[30] The structure was solved using direct methods with the SHELX-86 program.[31] The non-hydrogen atoms were refined with anisotropic thermal parameters. The hydrogen atoms were included in geometric positions and given thermal parameters equivalent to 1.2 times those of

the atom to which they were attached. The structure was refined on F^2 using SHELXL.[32] The final R values were $R1=0.0610$ and $wR2=0.1779$ for 1716 data with $I>2\sigma(I)$. The largest peak and hole in the final difference Fourier were 0.20 and -0.20 eÅ^{-3}.

Crystallographic data have been deposited at the Cambridge Crystallographic Data Center reference CCDC-176329 for peptide **2** and CCDC 184602 for peptide **6**.

Acknowledgements

We thank EPSRC and the University of Reading, UK for funds for the Image Plate System. A.B. acknowledges Department of Science and Technology, New Delhi, India for the grant No. SR/S5/OC-29/2003.

References and notes

1. (a) Dobson, C. M. *Nature* **2002**, *418*, 729–730; (b) Lynn, D. G.; Meredith, S. C. *J. Struct. Biol.* **2000**, *130*, 153–173; (c) Kelly, J. W. *Curr. Opin. Struct. Biol.* **1996**, *6*, 11–17; (d) Goldsbury, C.; Goldie, K.; Pellaud, J.; Seelig, J.; Frey, P.; Müller, S. A.; Kister, J.; Cooper, G. J. S.; Aebi, U. *J. Struct. Biol.* **2000**, *130*, 352–362; (e) Arvinte, T.; Cudd, A.; Drake, A. F. *J. Biol. Chem.* **1993**, *268*, 6415–6422; (f) Blanch, E. W.; Morozova-Roche, L. A.; Cochran, D. A. E.; Doing, A. J.; Hect, L.; Barron, L. D. *J. Mol. Biol.* **2000**, *301*, 553–563; (g) Spillantini, M. G.; Crowther, R. A.; Jakes, R.; Hasegawa, M.; Goedert, M. *Proc. Natl. Acad. Sci. U.S.A.* **1998**, *95*, 6469–6473.
2. (a) Baumeister, R.; Eimer, S. *Angew. Chem., Int. Ed.* **1998**, *37*, 2978–2982; (b) Lansbury, P. T., Jr. *Acc. Chem. Res.* **1996**, *29*, 317–321; (c) Rochet, J. C.; Lansbury, P. T., Jr. *Curr. Opin. Struct. Biol.* **2000**, *10*, 60–68; (d) Walsh, D. M.; Lomakin, A.; Benedek, G. B.; Condron, M. M.; Teplow, D. B. *J. Biol. Chem.* **1997**, *272*, 22364–22372; (e) Walsh, D. M.; Hartley, D. M.; Kusumoto, Y.; Fezoui, Y.; Condron, M. M.; Lomakin, A.; Benedek, G. B.; Selkoe, D. J.; Teplow, D. B. *J. Biol. Chem.* **1999**, *274*, 25945–25952; (f) Taubes, G. *Science* **1996**, *271*, 1493–1495.
3. (a) Scherzinger, E.; Sittler, A.; Schweiger, K.; Heiser, V.; Lurz, R.; Hasenbank, R.; Bates, G. P.; Lehrach, H.; Wanker, E. E. *Proc. Natl. Acad. Sci. U.S.A.* **1999**, *96*, 4604–4609; (b) Scherzinger, E.; Lurz, R.; Turmaine, M.; Mangiarini, L.; Hollenbach, B.; Hasenbank, R.; Bates, G. P.; Davies, S. W.; Lehrach, H.; Wanker, E. E. *Cell* **1997**, *90*, 549–558; (c) Chen, S.; Ferrone, F. A.; Wetzel, R. *Proc. Natl. Acad. Sci. U.S.A.* **2002**, *99*, 11884–11889.
4. (a) Prusiner, S. B. *Proc. Natl. Acad. Sci. U.S.A.* **1998**, *95*, 13363–13383; (b) Baldwin, M. A.; Cohen, F. E.; Prusiner, S. B. *J. Biol. Chem.* **1995**, *270*, 19197–19200; (c) Ng, S. B. L.; Doig, A. *Chem. Soc. Rev.* **1997**, *26*, 425–432.
5. (a) Petkova, A. T.; Ishii, Y.; Balbach, J. J.; Antzutkin, O. N.; Leapman, R. D.; Delaglio, F.; Tycko, R. *Proc. Natl. Acad. Sci. U.S.A.* **2002**, *99*, 16742–16747; (b) Tycko, R. *Biochemistry* **2003**, *42*, 3151–3159; (c) Balbach, J. J.; Ishii, Y.; Antzutkin, O. N.; Leapman, R. D.; Rizto, N. W.; Dyda, F.; Reed, J.; Tycko, R. *Biochemistry* **2000**, *39*, 13748–13759.
6. Puglielli, L.; Tanzi, R. E.; Kovacs, D. M. *Nat. Neurosci.* **2003**, *6*, 345–351.
7. (a) Kim, Y. S.; Randolph, T. W.; Manning, M. C.; Stevens, F. J.; Carpenter, J. F. *J. Biol. Chem.* **2003**, *278*, 10842–10850; (b) Taylor, D. L.; Allen, R. D.; Benditt, E. P. *J. Histochem. Cytochem.* **1974**, *22*, 1105–1112; (c) Lim, A.; Makhov, A. M.; Bond, J.; Inouye, H.; Conmors, L. H.; Griffith, J. D.; Erickson, W. B.; Kirschner, D. A.; Costello, C. E. *J. Struct. Biol.* **2000**, *130*, 363–370; (d) Azriel, R.; Gazit, E. *J. Biol. Chem.* **2001**, *226*, 34156–34161; (e) Gazit, E. *FASEB J.* **2002**, *16*, 77–83.
8. (a) Harper, J. D.; Wong, S. S.; Lieber, C. M.; Lansbury, P. T., Jr. *Chem. Biol.* **1997**, *4*, 119–125; (b) Walsh, D. M.; Lomakin, A.; Benedek, G. B.; Condron, M. M.; Teplow, D. B. *J. Biol. Chem.* **1997**, *272*, 22364–22372.
9. (a) Soto, C.; Sigurdsson, E. M.; Morelli, L.; Kumar, R. A.; Castano, E. M.; Frangione, B. *Nat. Med.* **1998**, *4*, 822–826; (b) Soto, C. *FEBS Lett.* **2001**, *498*, 204–207.
10. Venkatraman, J.; Shankaramma, C. S.; Balaram, P. *Chem. Rev.* **2001**, *101*, 3131–3152.
11. Gilead, S.; Gazit, E. *Angew. Chem., Int. Ed.* **2004**, *43*, 4041–4044.
12. Formaggio, F.; Bettio, A.; Moretto, V.; Crisma, M.; Toniolo, C.; Broxterman, Q. B. *J. Pept. Sci.* **2003**, *9*, 461–466.
13. (a) Karle, I. L.; Balaram, P. *Biochemistry* **1990**, *29*, 6747–6756; (b) Aravinda, S.; Shamala, N.; Das, C.; Sriranjini, A.; Karle, I. L.; Balaram, P. *J. Am. Chem. Soc.* **2003**, *125*, 5308–5315.
14. Bodanszky, M.; Bodanszky, A. *The Practice of Peptide Synthesis*; Springer: New York, NY, 1984; pp 1–182.
15. (a) Toniolo, C.; Palumbo, M. *Biopolymers* **1977**, *16*, 219–224; (b) Moretto, V.; Crisma, M.; Bonora, G. M.; Toniolo, C.; Balaram, H.; Balaram, P. *Macromolecules* **1989**, *22*, 2939–2944.
16. Dado, G. P.; Gellman, S. H. *J. Am. Chem. Soc.* **1994**, *116*, 1054–1062.
17. Blondelle, S. E.; Forood, B.; Houghten, R. A.; Peraz-Paya, E. *Biochemistry* **1997**, *36*, 8393–8400.
18. Haris, P. I.; Chapman, D. *Biopolymers* **1995**, *37*, 251–263.
19. Haldar, D.; Banerjee, A.; Drew, M. G. B.; Das, A. K.; Banerjee, A. *Chem. Commun.* **2003**, 1406–1407.
20. (a) Haldar, D.; Maji, S. K.; Sheldrick, W. S.; Banerjee, A. *Tetrahedron Lett.* **2002**, *43*, 2653–2656; (b) Haldar, D.; Maji, S. K.; Drew, M. G. B.; Banerjee, A.; Banerjee, A. *Tetrahedron Lett.* **2002**, *43*, 5465–5468.
21. Karle, I. L.; Banerjee, A.; Bhattacharjya, S.; Balaram, P. *Biopolymers* **1996**, *38*, 515–526.
22. Kamber, B. *Helv. Chim. Acta* **1971**, *54*, 398–422.
23. Abbenante, G.; March, D. R.; Bergman, D. A.; Hunt, P. A.; Garnham, B.; Dancer, R. J.; Martin, J. L.; Fairlie, D. P. *J. Am. Chem. Soc.* **1995**, *41*, 10220–10226.
24. Odake, S.; Okayama, T.; Obata, M.; Morikawa, T.; Hattori, S.; Hori, H.; Nagai, Y. *Chem. Pharm. Bull.* **1990**, *38*, 1007–1011.
25. Narita, M.; Ogura, T.; Sato, K.; Honda, S. *Bull. Chem. Soc. Jpn.* **1986**, *59*, 2433–2438.
26. Shin, C.; Ogawa, K.; Morooka, K.; Yonezawa, Y. *Chem. Lett.* **1989**, *18*, 459–462.
27. Balaram, H.; Sukumar, M.; Balaram, P. *Biopolymers* **1986**, *25*, 2209–2223.
28. Sheldrick, G. M. *SHELXS 97 Program for the Solution of Crystal Structures*; University of Gőttingen: Germany, 1997.
29. Sheldrick, G. M. *SHELXL 97 Program for the Refinement of Crystal Structures*; University of Gőttingen: Germany, 1997.
30. Kabsh, W. *J. Appl. Crystallogr.* **1988**, *21*, 916.
31. Sheldrick, G. M. *Acta Crystallogr., Sect. A: Fundam. Crystallogr.* **1990**, *46*, 467.
32. Sheldrick, G. M. *Program for Crystal Structure Refinement*; University of Gőttingen: Gőttingen, Germany, 1993.